

Supporting Information

Topological Effects in Isolated Poly[n]catenanes: Molecular Dynamics Simulations and Rouse Mode Analysis

Phillip M. Rauscher,[†] Stuart J. Rowan,^{†,‡,¶,§} and Juan J. de Pablo*,^{†,¶,||}

[†]*Institute for Molecular Engineering, the University of Chicago, Chicago, IL 60637, USA*

[‡]*Department of Chemistry, the University of Chicago, Chicago, IL 60637, USA*

[¶]*Institute for Molecular Engineering, Argonne National Laboratory, 9700 Cass Ave.,
Lemont, IL 60439, USA*

[§]*Chemical Sciences and Engineering Division, Argonne National Laboratory, 9700 Cass
Ave., Lemont, IL 60439, USA*

^{||}*Materials Science Division, Argonne National Laboratory, 9700 Cass Ave., Lemont, IL
60439, USA*

E-mail: depablo@uchicago.edu

Model and Methods

Poly[n]catenanes were simulated using the coarse-grained bead-spring model of Kremer and Grest,²⁵ which has been used extensively in the literature, including several applications to interlocking molecular architectures.^{10,14,26-29} All beads have mass M , diameter σ , and

interact with one another via a purely-repulsive Lennard-Jones (LJ) potential:

$$U(r) = 4\epsilon \left[\left(\frac{\sigma}{r}\right)^{12} - \left(\frac{\sigma}{r}\right)^6 + \frac{1}{4} \right] \tag{S1}$$

where r is the separation distance between the two beads and the interaction is cut off at $r_c = 2^{\frac{1}{6}}\sigma$. Neighboring beads within covalently-bound segments are connected to one another with a finitely extensible non-linear elastic (FENE) potential:

$$U_{FENE}(r) = -\frac{1}{2}kR_0^2 \ln \left[1 - \left(\frac{r}{R_0}\right)^2 \right] \tag{S2}$$

with the maximum separation $R_0 = 1.5\sigma$ and stretching constant $k = 30\epsilon$. To alter chain stiffness, a cosine bond-angle bending potential was used with the form:

$$U_{bend}(\theta) = k_\theta (1 + \cos \theta) \tag{S3}$$

where θ is the angle between adjacent bonds in the molecules, and the bending constant k_θ is an adjustable parameter used to study flexible ($k_\theta = 0.0$), semi-flexible ($k_\theta = 1.5$), and rigid ($k_\theta = 10.0$) chain segments. The simulation cell was a large cubic box with edge length much longer than the end-to-end distance of the polymers studied and the molecules were allowed to drift freely. Equations of motion were integrated for 10^9 production time steps using a velocity-Verlet algorithm and a time step of 0.005τ where $\tau = \sigma \left(\frac{M}{\epsilon}\right)^{\frac{1}{2}}$ is the Lennard-Jones unit of time. All relaxation times (rates) are reported in terms of τ ($1/\tau$). Constant temperature and the effect of solvent fluctuations were included through the use of a Langevin heat bath with temperature $T = \epsilon/k_B$ and damping constant $\gamma = 0.5\tau^{-1}$. All simulations were conducted using the GPU-accelerated, Python-wrapped MD engine DASH.³¹ Poly[n]catenanes were prepared by placing n circular molecules of m beads along the x -axis of the simulation box at distances/orientations ensuring an interlocking structure. The molecules were then equilibrated for 2×10^8 time-steps using the parameters described

above. This equilibration period is roughly 10 times longer than the longest Rouse time observed for any polymer in the study ($\sim 10^5\tau$), ensuring that the systems are completely decorrelated from their initial states prior to production simulations. Particle coordinates were harvested every 200 time steps (1.0τ) for analysis. To analyze the rapid relaxations of individual macrocycles and small ring/linear polymers, shorter simulations of 2×10^7 time steps were performed and particle coordinates were harvested every 25 time steps (0.125τ). To ensure adequate sampling of the three longest Rouse modes in the poly[n]catenanes, 10-20 independent simulations of 10^9 time steps were performed for ring sizes of $m = 10, 15, 20$, and 30, calculating the Rouse modes on-the-fly every 2000 time-steps.

To determine how inertia impacts the systems, we conducted some additional simulations using an over-damped Brownian dynamics model and an Euler-Maruyama integration scheme. The relaxation rates W_p^{eff} were not qualitatively different for either linear polymers or poly[n]catenanes. However, the stretching exponents β_p for linear polymers did not increase to values greater than one at high mode number as in the inertial case; instead, they remained relatively constant in the range 0.8-1.0, in agreement with results from unentangled melts.¹⁷ The β_p for poly[n]catenanes were mostly unchanged and still significantly reduced compared to the linear case. In short, the presence or absence of inertia does not alter the results in a meaningful way.

Rouse Theory and Calculation

In the Rouse theory of polymer dynamics,¹⁶ linear macromolecules are represented as a series of N beads connected by harmonic springs with spring constant $\frac{3k_B T}{b^2}$, where b^2 is the mean-squared segment length. The real, symmetric matrix describing the bonded interactions between neighboring beads can be diagonalized to yield a set of N eigenvectors

with associated eigenvalues given by:

$$\lambda_p = 4 \sin^2 \left(\frac{p\pi}{2N} \right) \quad (\text{S4})$$

The eigenvectors constitute the columns of an orthogonal matrix which can be multiplied with the set of monomer coordinates to yield a series of normal modes, given by the following formula (for linear chains):

$$\mathbf{X}_p = \left(\frac{2}{N} \right)^{1/2} \sum_{i=1}^N \mathbf{R}_i \cos \left[\frac{p\pi}{N} \left(i - \frac{1}{2} \right) \right] \quad (\text{S5})$$

where \mathbf{X}_p is the p^{th} Rouse mode ($p > 0$), and \mathbf{R}_i is the position of the i^{th} bead in the polymer. The zeroth mode corresponds to the center-of-mass of the polymer and has been ignored in this letter. The resulting Langevin equations for all \mathbf{X}_p indicate that the autocorrelation functions (ACFs) of the Rouse modes (which describe relaxations of segments of N/p beads) decay as simple exponentials:

$$\frac{\langle \mathbf{X}_p(t) \cdot \mathbf{X}_p(0) \rangle}{\langle \mathbf{X}_p^2 \rangle} = \exp \left(-\frac{t}{\tau_p} \right) \quad \text{with} \quad \tau_p^{-1} = \frac{12k_B T \sin^2(p\pi/2N)}{\zeta b^2} \quad (\text{S6})$$

where ζ is the monomeric drag coefficient. Scaling the inverse relaxation time by the corresponding eigenvalue yields the monomeric relaxation rate which is independent of mode number:

$$W = \frac{1}{\lambda_p \tau_p} = \frac{3k_B T}{\zeta b^2} \quad (\text{S7})$$

In practice, a stretched exponential form (a.k.a. KWW function) describes the behavior of the ACFs much better:

$$\frac{\langle \mathbf{X}_p(t) \cdot \mathbf{X}_p(0) \rangle}{\langle \mathbf{X}_p^2 \rangle} = \exp \left[-\left(\frac{t}{\tau_p} \right)^{\beta_p} \right] \quad (\text{S8})$$

The integral of the ACF, which defines an effective relaxation time, is given in terms of the gamma function, $\tau_p^{\text{eff}} = (\tau_p/\beta_p)\Gamma(1/\beta_p)$. Substituting this value into Eq. S7 above yields

the effective monomeric relaxation rate:

$$W_p^{eff} = \frac{1}{\tau_p^{eff} \lambda_p} \quad (\text{S9})$$

Note that following standard practice in the literature,¹⁷⁻²⁰ the *ideal* eigenvalues (given by Eq. S4) are used in Eq. S9. When this approach is taken, any deviations from a constant, mode-independent value correlate with deviations from ideal chain dynamics.

For ring polymers, the matrix describing the bonded interactions between beads has the same form, but different boundary conditions. The resulting eigenvalues are the same as in the linear case, but the odd modes vanish and even modes with $p \geq 2$ have a degeneracy of two. Thus, each eigenvalue corresponds to a two-dimensional eigenspace. A set of eigenvectors can then be written:

$$\mathbf{X}_p = \begin{cases} \left(\frac{2}{N}\right)^{1/2} \sum_{i=1}^N \mathbf{R}_i \cos\left(\frac{p\pi i}{N}\right) & \text{for } p = 2, 4, \dots, \frac{N}{2} - 2 \\ \left(\frac{2}{N}\right)^{1/2} \sum_{i=1}^N \mathbf{R}_i \sin\left(\frac{p\pi i}{N}\right) & \text{for } p = 2, 4, \dots, \frac{N}{2} - 2 \\ \left(\frac{1}{N}\right)^{1/2} \sum_{i=1}^N \mathbf{R}_i (-1)^i & \text{for } p = \frac{N}{2} \end{cases} \quad (\text{S10})$$

As in the case of linear chains, the zeroth mode corresponds to the polymer center of mass and is not considered here. Also, the third row of Eq. S10 does not apply for odd N . These results are equivalent to those given by Ceriotti et al. for the thermostating of ring polymers in path integral molecular dynamics.³² A detailed presentation of the Rouse theory for ring polymers in discrete form - as well as the continuous limit - can be found in ref. 21. Clearly, the eigenvectors within each eigenspace can be related to one another by a shift in the indexing of the monomers (although not necessarily by an integer value). However, just as the choice of the initial versus final chain end in linear polymers is arbitrary, the indexing in a ring polymer is also arbitrary. Therefore, by symmetry arguments, it will not affect the

averages of any quantities related to the Rouse modes, including the ACFs. Thus, only a single mode is considered for each eigenspace; in analogy with the coordinate transformation for linear chains and following previous works, the cosine transformation is chosen (first line of Eq. S10).

For the highest modes of the linear polymer with $m_{eff} = 3$, the ACF shows some oscillatory behavior, presumably due to the increased importance of bonded interactions at short length scales. Since τ_p^{eff} is defined as the integral of the ACF, a stretched exponential function overestimates the relaxation time in this regime since it cannot account for negative values. Empirically, the following function is able to fit the data well:

$$\frac{\langle \mathbf{X}_p(t) \cdot \mathbf{X}_p(0) \rangle}{\langle \mathbf{X}_p^2 \rangle} = \{\cos[A \ln(t + 1)]\} \times \exp \left[\left(\frac{t}{\tau_p} \right)^{\beta_p} \right] \quad (\text{S11})$$

where A is an additional fitting parameter. This can be numerically integrated to yield a more correct value of τ_p^{eff} . This functional form was chosen on a purely empirical basis and no physical significance should be attached to it. For modes where Eq. S11 is used to fit the ACF, the features of the stretching exponents, β_p , are not analyzed.

Throughout this letter, we have focused on the Rouse modes with $p \geq 1$ as these describe the internal relaxations of the molecule. As mentioned earlier, the zeroth mode corresponds to the polymer center-of-mass, so there is no "relaxation" *per se*, only diffusive motion. Since our simulations do not account for hydrodynamic effects, the macromolecules should obey normal diffusive behavior with the mean-squared displacement proportional to t^1 , which is clearly seen for all poly[n]catenane species in Fig. S3. Furthermore, all polymers in this letter have diffusion constants which agree quantitatively with the usual prediction $D = \frac{k_B T}{N\zeta}$, as seen in Fig. S4.

A key aspect of the Rouse theory is that the modes are statistically independent. This orthogonality allows one to interpret mode relaxations as dynamical processes with well-defined length scales (N/p) and enables the calculation of various material functions, such

as shear stress relaxation modulus and dynamic structure factor. However, if there exist significant cross-correlations between modes, such analysis are invalid and the Rouse modes no longer have a straight-forward physical interpretation. Therefore, it is important to assess whether or not the Rouse modes are indeed orthogonal in our systems. This is particularly important since some authors have found significant cross-correlations at high mode number for entangled melts of linear polymers i.e. in the presence of topological interactions.³³ Following previous authors,^{34,35} we assess the orthogonality using a normalized correlation product:

$$\chi_{pq} = \frac{|\langle \mathbf{X}_p \cdot \mathbf{X}_q \rangle|}{\sqrt{\langle \mathbf{X}_p^2 \rangle \langle \mathbf{X}_q^2 \rangle}} \quad (\text{S12})$$

which takes on a value of one for $p = q$ and should be zero for $p \neq q$ if the modes are orthogonal. We compute these quantities for both sets of Rouse modes considered. For the modes of individual rings within pol[n]catenanes, the mode $p = 2$ shows some coupling with the other modes, with the largest correlations reaching $\chi_{pq} \approx 0.1$. However, since the amplitude of the lower modes are much larger than the rest, the sum total of un-normalized cross-correlations is still 2 orders of magnitude smaller than the self correlation in the low- p regime, so these couplings are not likely to affect the relaxation behavior meaningfully in the region of interest. Figure S5 shows the cross-correlations (Eq. S12) between macrocycle modes in the form of a heat map for poly[n]catenanes with $m = 30$ and $m = 100$ beads per macrocycle. For the second set of Rouse modes, corresponding to the entire poly[n]catenane chain or a linear analogue, we observe non-zero coupling between pairs of modes with both even or both odd mode numbers. The same trend has been observed repeatedly in the literature and results in a checker-board pattern in the resulting cross-correlation heat map (Figure S6). In agreement with literature results,³³⁻³⁵ the cross-correlations are always at least 1-2 orders of magnitude smaller than the self-correlation, suggesting that the Rouse modes are indeed orthogonal to within reasonable approximation. In general, poly[n]catenanes of all ring sizes exhibit larger couplings at low mode number than do the linear analogues. However, at higher mode

number, the couplings are suppressed and the modes become *more* orthogonal; this is clearly seen in the resulting correlation heat map, which shows much more yellow/orange coloring in the lower left (low mode number) than in the upper right (high mode number). So while the Rouse analysis is indeed applicable to the entire polymer, the results will be particularly useful at high mode number, which is where the most unusual dynamics are observed. In summary, we may conclude that cross-correlations between modes cannot be responsible for the qualitatively different relaxation behavior of poly[n]catenanes.

Static Properties

Here we present a few selected static properties of poly[n]catenanes and their linear counterparts. Since this letter focuses on the dynamical behaviors, we discuss only those properties which are useful for understanding and interpreting the dynamics. A more detailed analysis of the structural characteristics has previously been performed by Pakula and Jeszka.¹⁵ Table S2 shows various elementary quantities including mean segment length between effective monomers (b), radius of gyration (R_g), and end-to-end distance (R_{ee}) for poly[n]catenanes and linear counterparts. Although mean effective bond lengths differ by at most 2% between architectures, linear polymers have smaller end-to-end distance and radius of gyration, which is probably caused by local chain swelling and excluded volume effects. By design, macrocycles and the effective monomers in linear analogues have the same segmental volume (b^3), but the macrocycles contain many more beads ($m > 3 \times m_{eff}$). Because of this increased bead density, one may expect poly[n]catenanes to be more strongly impacted by excluded volume and therefore stiffer than linear polymers. This leads to physically larger/longer molecules, which slows down the large length-scale dynamics; in the main text, this expectation is borne out as linear chains tend to relax 50-80% faster than poly[n]catenanes at the lowest modes. The same trend is evidenced by the local structure of the polymers.

To understand local chain structure, two additional quantities are calculated: the mean-squared amplitudes of the Rouse modes and the mean-squared internal distances between effective monomers. Physically, these quantities both represent the size of sub-chains, but are calculated according to different means. For ideal chains, the Rouse mode amplitudes are given by

$$\langle \mathbf{X}_p^2 \rangle = \frac{3k_B T}{k\lambda_p} = \frac{b^2}{\lambda_p} \quad (\text{S13})$$

where k is the spring constant between neighboring beads. For chains with excluded volume effects, the following scaling relation will hold in the asymptotic limit:³⁵

$$\lambda_p \langle \mathbf{X}_p^2 \rangle \sim \left(\frac{N}{p} \right)^{2\nu-1} \quad (\text{S14})$$

where ν is the Flory exponent. The scaled amplitudes for poly[n]catenanes and linear analogues as a function of n/p are shown in Figs. S7 and S8, respectively. In all cases, there is a positive slope at the largest length scales which suggests that the chains are not long enough to reach the asymptotic limit and are therefore in some intermediate or crossover regime. The values for poly[n]catenanes generally span a wider range than linear counterparts, indicating that they are subject to greater local stiffness effects. The linear polymers also appear to level off more quickly at higher values of n/p , while the poly[n]catenanes seem slower to reach their asymptotic limit.

The scaled Rouse mode amplitudes for individual macrocycles within poly[n]catenanes can also be calculated and compared to free ring polymers and linear chains. The results for macrocycles of size $m = 100$ and $m = 30$ are shown in Figs. S9 and S10, respectively, and the results are qualitatively similar. At high mode numbers (short length scales), the mode amplitudes vary according to the number of threadings, with poly[n]catenane chain centers having the lowest amplitudes, followed by chain ends, and then free polymers. In this regime, the dependence on N/p is identical for all systems. At the lowest mode, however, the situation is reversed, with all three cyclic systems having amplitudes larger than the linear

polymer. Furthermore, the magnitude of the modes now increases with increased threading, contrary to the situation at high mode number. These data suggest that ring polymers and catenane macrocycles are expanded at large length scales compared to linear chains, and that the mechanical bonds magnify the effect.

The mean-square internal distances between effective monomers are another set of data which describe the internal structure of polymer chains. They are qualitatively similar to the Rouse mode amplitudes in that they quantify the size of sub-chains within the molecule. For a polymer with N effective monomers, these data are calculated according to:

$$R^2(n) = \frac{1}{N-n} \sum_{i=1}^{N-n} \langle (\mathbf{R}_{i+n} - \mathbf{R}_i)^2 \rangle \quad (\text{S15})$$

where $n > 0$, \mathbf{R}_i is the position of effective monomer i , and the brackets $\langle \dots \rangle$ indicate an ensemble average. The quantity R^2 is typically divided by n so that ideal random walk statistics correspond to a constant value. Figures S11 and S12 show these data for linear polymers and poly[n]catenanes, respectively. As expected, all polymers are locally swollen at short length scales, showing increasing values before leveling off at higher n . However, it is clear from this data that linear polymers are considerably *less* expanded than poly[n]catenanes, which is presumably a consequence of the lower bead density within each segment volume. The transition to "ideal" statistics at $n \sim 20$ rings in the poly[n]catenanes is likely the result of increased flexibility/mobility at the chain ends. Further normalization by the mean-squared segment length $b^2 \equiv R^2(1)$, allows for comparison of chain structure across architectures, as shown in Fig. S13. In the case of linear chains with various values of m_{eff} , all curves converge. However, for poly[n]catenanes, smaller macrocycles lead to greater relative swelling, which would indicate enhanced excluded volume effects at short length scales and greater overall stiffness, consistent with the observations from the Rouse mode amplitudes. These data also support the conclusion that these polymers are not large enough to reach the asymptotic scaling limit. Beyond these features, there are no other anomalies associated

with poly[n]catenane structure at any length scale (so far as effective monomers are concerned). Therefore, one would expect the dynamical properties at short length scales to be consistent with those of an ordinary polymer with excluded volume. However, as described in the main text, there are indeed *qualitative* differences in dynamics at short length scales between poly[n]catenanes and linear polymers. We will show later that such differences cannot be understood in terms of the static scaling properties, which are qualitatively *similar* for all architectures considered.

Scaling of Relaxation Rates

Depending on the size of the effective monomer, W_p^{eff} as determined from Eq. S9 can be spread over 1-2 orders of magnitude, making comparisons between the various polymers difficult (see Figs. 3a, S14). Therefore, some method of scaling these spectra must be introduced. A straightforward approach is to leverage Eq. S7, which indicates that the relaxation rates should be inversely proportional to b^2 (which indicates the segment size) and ζ , the drag coefficient of the monomer. This relationship suggests that multiplying W_p^{eff} by these quantities (or values directly proportional to them) would allow for comparisons between polymers of different molecular weight and monomer size. In a Langevin dynamics simulation, the drag coefficient for a relatively small molecule will be directly proportional to the number of beads in the molecule so that the monomeric drag is proportional to either m or m_{eff} for poly[n]catenanes and linear polymers, respectively. Meanwhile, mean values of b^2 can be obtained directly from simulation trajectories. Accordingly, a scaled relaxation rate is defined as:

$$W_p^{scaled} = m \langle b^2 \rangle W_p^{eff} \quad (\text{S16})$$

where the brackets indicate an average obtained from the simulation, and m and b^2 depend on the architecture in question. Applying this formula to the relaxation rates for both linear polymers and poly[n]catenanes, the spectra are now much more comparable (Figs. S15

and S16). Two features are immediately apparent: 1) the curves show a dependence on p at low mode numbers, suggesting that they do not obey ideal Rouse dynamics, and 2) the relaxation rates increase monotonically with the size of the effective monomer. Both of these observations may be understood in terms of excluded volume effects, which can be included using a dynamical scaling argument.

To begin this scaling argument, a similar analysis by Doi and Edwards¹ is summarized, considering only the case of linear polymers for the time being. In the Rouse theory, the longest relaxation time for a group of N segments is given by:

$$\tau_N \propto \frac{\zeta b^2 N^2}{k_B T} \quad (\text{S17})$$

Using a dimensional analysis, an expression can be crafted which contains the same physical quantities as Eq. S17, but assumes no particular dependence on N , so that it may be applied to non-ideal polymers:

$$\tau_N \propto \frac{\zeta b^2}{k_B T} f(N) \quad (\text{S18})$$

The fraction has units of time, while the function $f(N)$ is dimensionless. By lumping together groups of κ segments, the following scaling transformation is introduced:

$$N \rightarrow N/\kappa \quad b \rightarrow \kappa^\nu b \quad \zeta \rightarrow \kappa \zeta \quad (\text{S19})$$

where ν is the scaling exponent. Since the relaxation time must be unaffected by the scaling (i.e. independent of κ), insertion of Eq. S19 into Eq. S18 yields the form of $f(N)$:

$$\tau_N \propto f(N) \propto N^{2\nu+1} \quad (\text{S20})$$

This result was first noted by de Gennes³⁶ and confirmed by simulations^{37,38} some time ago. Now roughly speaking, the p^{th} Rouse mode describes relaxations of segments of N/p beads. In keeping with the self-similar nature of polymers, it is assumed that Eq. S20 also holds for

sub-chains, so that the Rouse relaxation times may be written as:

$$\tau_p \propto \left(\frac{N}{p}\right)^{2\nu+1} \quad (\text{S21})$$

This same (approximate) scaling has been proposed before by Panja *et al.*³⁵ Now for small p , the eigenvalues are approximated as $\lambda_p \sim (p/N)^2$ (recall that we have used the *ideal* eigenvalues given by Eq. S4 in the calculation of W_p^{eff}). This relation, along with Eqs. S7 and S21, indicates that the relaxation rates scale as

$$W \sim \left(\frac{N}{p}\right)^{1-2\nu} \quad (\text{S22})$$

in the small- p range. Later, it will be shown that for linear polymers, $W_p^{eff} \sim p^{-0.12}$, indicating a scaling exponent of 0.56, which is consistent with good solvent conditions (see Fig. S17).

One may use similar arguments to understand why the scaled relaxation rates increase as the effective monomer size increases. Consider the density of beads within the effective monomer, $\rho \sim m_{eff}/b^3$. Since $b \sim m_{eff}^\nu$, this density decreases with increasing m_{eff} in a good solvent. Smaller bead densities allow for greater overlap between effective monomers, which reduces the relative importance of excluded volume effects, leading to faster dynamics in analogy with Eq S20. To quantitatively account for this effect, the dynamical scaling argument is used again. In particular, it is clear that the relaxation time for a given chain segment should not depend on the level of discretization, i.e. m_{eff} . However, such a dependence is introduced into the relaxation rates W_p^{eff} through the eigenvalues λ_p in Eq. S9, since different discretizations yield different values of n/p and therefore different eigenvalues. Furthermore, the values of ζ and b^2 also depend on m_{eff} as already discussed. To understand the effect of this discretization, consider a chain (or sub-chain) of N monomers with a relaxation time τ_N which obeys Eq. S20. For a given effective monomer size m_{eff} , one may

write:

$$\left(\frac{n}{p}\right)_{eff} = \frac{N}{m_{eff}} \quad (\text{S23})$$

which represents the number of effective monomers in the segment for a given discretization. Using Eqs. S7, S16, S20, and S23, along with the small- p approximation for λ_p and the relation $b \sim m_{eff}^\nu$, one finds:

$$W_p^{\text{scaled}} \propto \left(\frac{N}{m_{eff}}\right)^{1-2\nu} \quad (\text{S24})$$

In good solvents, the scaling exponent will be greater than 1/2, so that W_p^{scaled} increases monotonically with m_{eff} , which is indeed the observed behavior. Eq. S24 indicates that one may correct the relaxation spectra produced by Eq. S16 by multiplying the values of W_p^{scaled} by the denominator of the right-hand side of Eq. S24. The final result is:

$$\text{Scaled } W_p^{eff} = m_{eff}^{2-2\nu} \times \langle b^2 \rangle \times W_p^{eff} \quad (\text{S25})$$

For large length scales (low mode number), the resulting spectra should collapse onto a master curve for traditional linear polymers. Alternatively, one may exploit the power law relationship by plotting W_p^{scaled} (Eq. S16) as a function of $(n/p) \times (1/m_{eff})$, noting that on a log-log plot, vertical and horizontal shifts of power law functions are effectively the same thing. This approach provides a convenient test for the scaling procedure since it does not require any prior knowledge concerning the value of ν ; rather, the value may be inferred if the spectra collapse onto a master curve (provided it is a straight line). The result is indeed a master curve at large length scales, as shown for linear polymers in Fig. S17. The slope of the linear portion at low mode number reveals the scaling exponent, $\nu = 0.56$, consistent with good solvent conditions. This representation successfully accounts for excluded volume effects introduced by the effective monomer size, allowing for comparisons between polymers with different effective monomer sizes. However, this approach cannot be expected to yield perfect agreement in all scenarios. In particular, for any real polymer chain, the effective value of the scaling exponent will be non-constant at low molecular weight, which

will introduce discrepancies into the results; clearly such errors are not too large, especially at low mode number. Having developed a scaling methodology in the context of linear polymers, the more delicate problem of poly[n]catenane systems must now be addressed.

Many of the assumptions invoked in the above argument cannot be readily applied to poly[n]catenanes, in which the number of beads in an effective monomer (i.e. macrocycle), m , has a true physical meaning and is not simply a parameter of the analysis. In general, the scaling behaviors of poly[n]catenanes will be quite complicated. One can immediately envision *at least* two different types of scaling: a familiar one involving changes in the number of rings, and a new one involving changes in the *size* of the rings. In general, the latter will violate self-similarity, thus precluding any straightforward scaling analysis. For instance, it would be unreasonable to assume *a priori* that a [100]catenane with $m = 5$ will relax on the same time scale as a [5]catenane with $m = 100$ just because they have the same molecular weight. Such an assumption becomes even more dubious when the entanglement effects are considered.

However, the simulations conducted here have indicated that for reasonably large catenane segments, the relaxation times are not strongly dependent on the size of the macrocycles, provided that the molecular weights are comparable. For example, when $n = 25$, the values of τ_1 for $m = 10$ and τ_3 for $m = 30$ both describe relaxations of ~ 250 beads and differ by only $\sim 8\%$. As one might expect, the longer of the relaxation times corresponds to the system with the smaller macrocycles, i.e. the one with the greater density of mechanical bonds. Perhaps for the macrocycle and catenane sizes studied here, the polymer can be thought of as a homogeneous coil of beads, allowing one to neglect the local structure of the chain at large length scales. In this picture, the two varieties of scaling discussed above are effectively the same. Naturally, in the limits of either very large or very small macrocycles, this behavior would not hold. To proceed, we fit the scaling of b vs. m to a power law, finding that $\nu = 0.658$ in this regime (Fig. S18), somewhat larger than the ordinary good-solvent value, which is unsurprising since the macrocycles are rather small. The scaled relaxation

spectra are then calculated according to:

$$\text{Scaled } W_p^{eff} = m^{0.684} \times \langle b^2 \rangle \times W_p^{eff} \quad (\text{S26})$$

Having corrected for the excluded volume effect, the relaxation spectra for poly[n]catenanes collapse onto a master curve at low mode number, similar to linear polymers. With this scaling procedure in hand, the dynamics of catenanes with different macrocycle sizes can be properly compared to study the effect of the mechanical bond (Fig. 3b).

It is worthwhile to comment on the physical significance of this scaling procedure and the limits of its interpretation. The excluded volume arguments used above are only truly valid in the large-scale asymptotic limit and even then are merely approximations. As discussed in the previous section, the poly[n]catenanes studied here are not large enough to reach this regime, at least in terms of static properties. While the connection between static and dynamic scaling is not well defined, it can be safely assumed that these polymers (and indeed their linear analogues) are in a crossover regime and therefore do not have a well-defined value of the scaling exponent, ν , which can be formally applied to a dynamical scaling analysis. Therefore, the excluded volume arguments, whose correctness is evidenced only by their ability to converge the spectra, should not be taken as important results in this letter. However, this does not affect the key findings of this letter: if the effects of excluded volume were completely ignored and the spectra were only scaled according to segment size and monomer drag (Eq. S16), the qualitative differences associated with decreasing ring size would still be apparent, as demonstrated by Fig. S16. In fact, if we have eschewed *any* theoretical basis for scaling the spectra and had simply shifted or normalized them in an *ad hoc* manner, the same conclusions would have been reached. The scaling procedure therefore represents only a means to rationalize the *quantitative* differences between the spectra of poly[n]catenanes with various ring sizes, but it does not impact the *qualitative* distinctions, which are the key findings.

We also wish to emphasize the point that the n/p dependencies at high mode numbers (short length scales) could *not* be expected merely on the basis of non-asymptotic behavior. For a swollen polymer chain, the effective spring constant between segments is increased, leading to faster dynamics. This effect can be easily seen in the case of linear polymers: various static properties (see Figs. S7 and S11) show that the chains are swollen at small length scales and accordingly show accelerated dynamics in this regime (Fig. S14). One could account for these local stiffness effects by recognizing that (in the ideal case) both the Rouse relaxation time and the mean-squared mode amplitudes are inversely proportional to the effective spring constant, suggesting that the quantity $W_p^{eff} \cdot \lambda_p \langle X_p^2 \rangle$ (an effective mobility) should be constant for all modes. Based on common scaling relations, this result should also hold in the large-length scale limit for chains with excluded volume. This sort of analysis combining static and dynamic simulation results has been attempted by many researchers^{20, 33, 39–42} with mixed results. In particular, Colmenero and coworkers^{20, 41, 42} have repeatedly shown that local stiffness *cannot* explain the deviations from ideal behavior at high mode number and a mode-dependent friction coefficient must be introduced. A similar observation was made in polymer melts and glasses employing the same molecular model used here.⁴⁰ However, it is unclear what physical factors influence this effective friction and in what way, precluding further analysis. But even if we applied such a procedure, it would not affect the results of this letter. As discussed above, poly[n]catenanes are swollen at short length scales, as seen through the static properties (Figs. S8 and S12). However, the relaxation rates do *not* show an upturn at high mode number as the linear polymers do. In fact, for the smallest ring sizes $m = 10$ and 15 , the relaxation rates actually *decrease* at the shortest length scales, where the chains are the *most* swollen and should therefore be *most* accelerated! Therefore, applying this kind of analysis would only emphasize the differences between the various poly[n]catenanes at short length scales. In summary, even though these poly[n]catenanes are in a crossover scaling regime (i.e. not in the asymptotic limit), this cannot explain the differences in relaxation behavior which occur at small length

scales along the polymer backbone.

Finally, the methodology for comparing poly[n]catenanes to their linear analogues is discussed. The arguments presented above allow one to correct for excluded volume effects for both linear polymers and poly[n]catenanes separately, but they do not readily indicate a basis for comparing the two species to one another. Indeed, this analysis is based on the fact that molecules with the same architecture and molecular weight must relax on the same time scale, no matter the level of discretization or coarse-graining. However, this does not hold across polymer architectures: poly[n]catenanes relax much faster than linear polymers of the same molecular weight. This is not a particularly interesting result since the poly[n]catenanes are far smaller in size than the linear polymers and therefore *should* relax faster; the same phenomenon is well-known in the context of ring polymers. It is for this reason that linear polymers and poly[n]catenanes are compared on the basis of segment length, as described in the main text. Only Eq. S16 is applied, with the understanding that poly[n]catenanes possess greater excluded volume effects than their linear counterparts, and that these effects are not controlled for. This limitation is unimportant. As demonstrated above, any scaling arguments used to account for excluded volume effects will result merely in a vertical shift of the spectra, which does not change the *qualitative* character of the data. Indeed, the key findings of this study are those qualitative differences in dynamics associated with the novel poly[n]catenane architecture.

Additional Figures and Tables

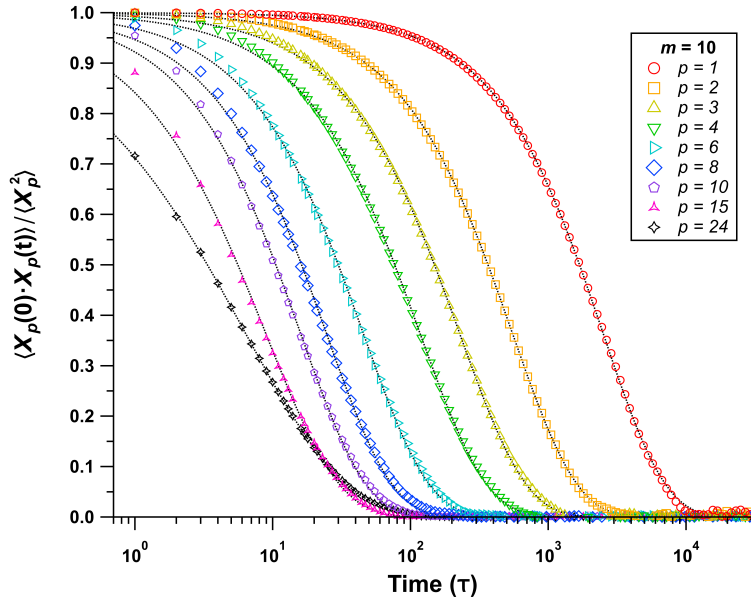


Figure S1: Representative subset of normalized Rouse mode ACFs for poly[n]catenane with $n = 25$ and $m = 10$. Points are simulation data; dotted lines are fits to Eq. S8. The $p = 24$ curve crosses over the $p = 15$ curve at $t \sim 25\tau$ due to the reduction in β_p at high mode number (cf. Fig. 5).

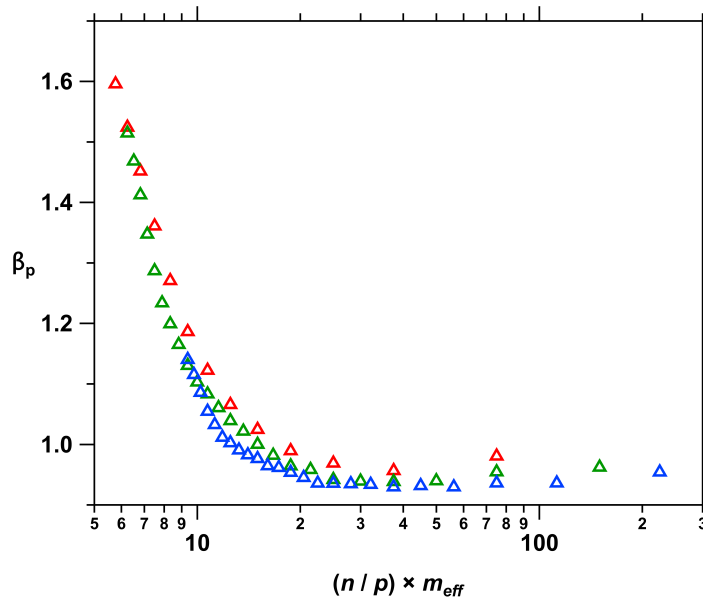


Figure S2: Stretching exponents for linear polymers plotted against an absolute length scale (i.e. a specific number of beads). Deviations from ideal Rouse behavior occur on the scale of ~ 10 beads.

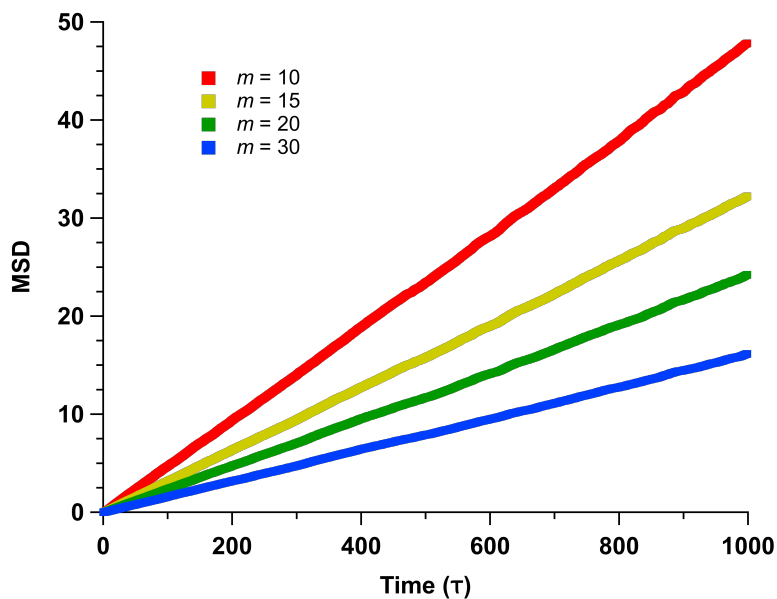


Figure S3: Mean squared displacements of poly[n]catenane centers of mass as a function of time for various ring sizes (m). All polymers diffuse normally with $\text{MSD} \propto t$

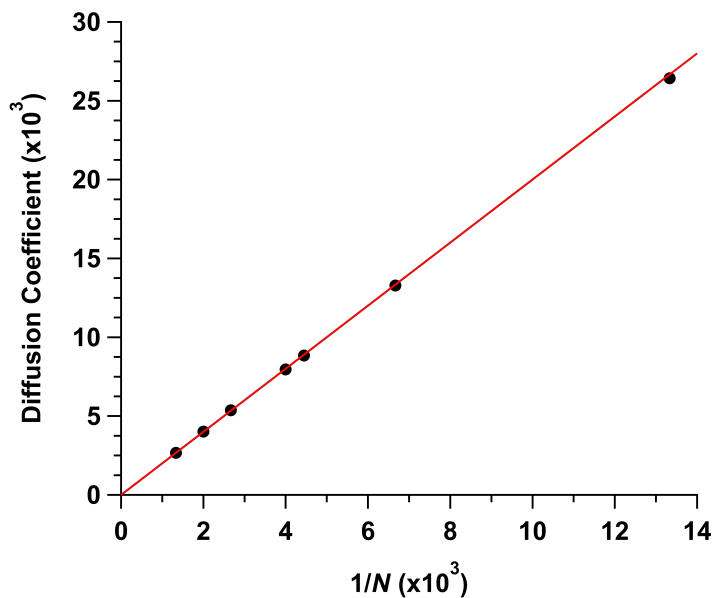


Figure S4: Diffusion coefficient as a function of inverse molecular weight, $1/N$. The red line shows the expected dependence based on simulation parameters.

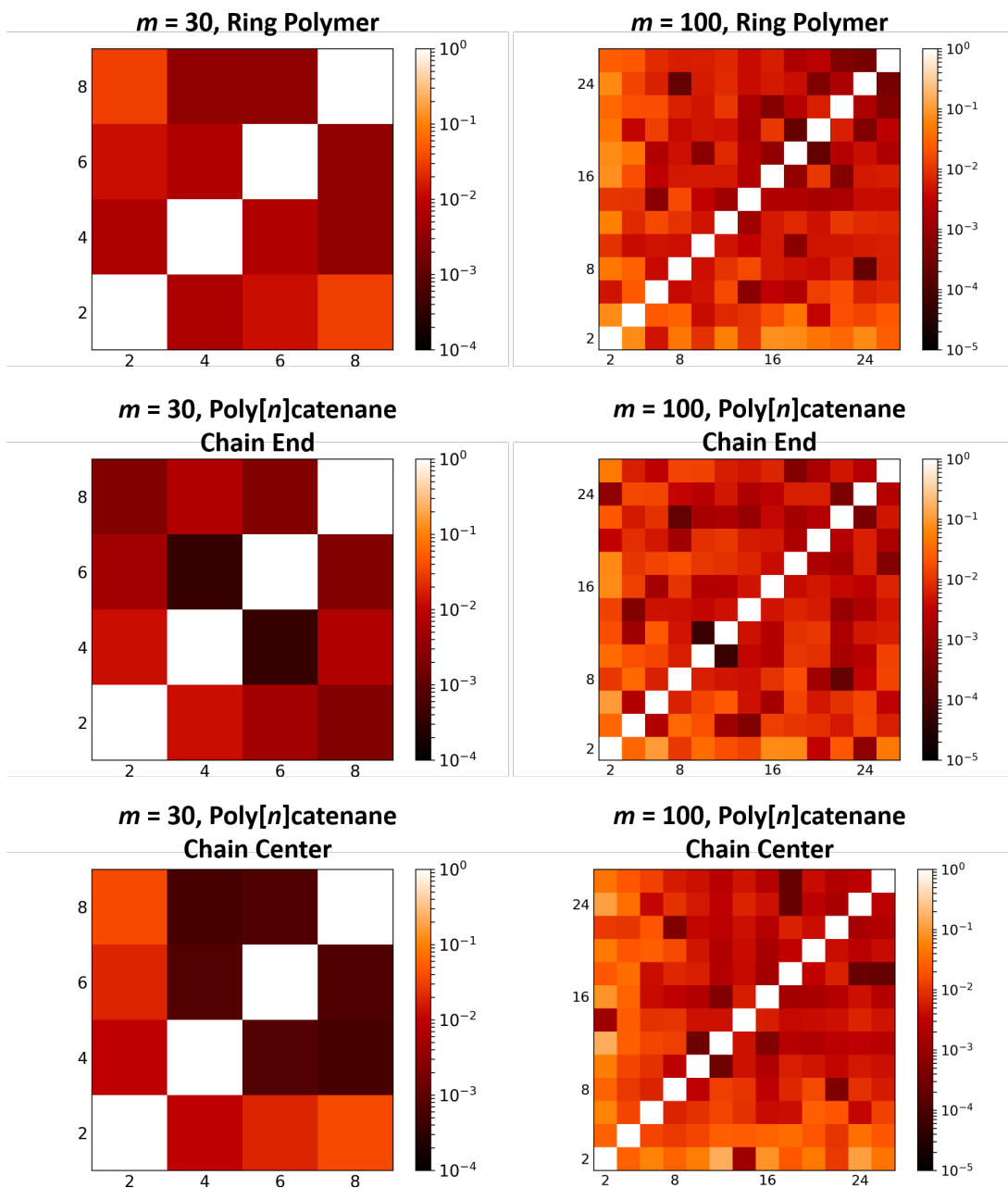


Figure S5: Normalized correlations between Rouse modes for macrocycles within poly[n]catenanes.

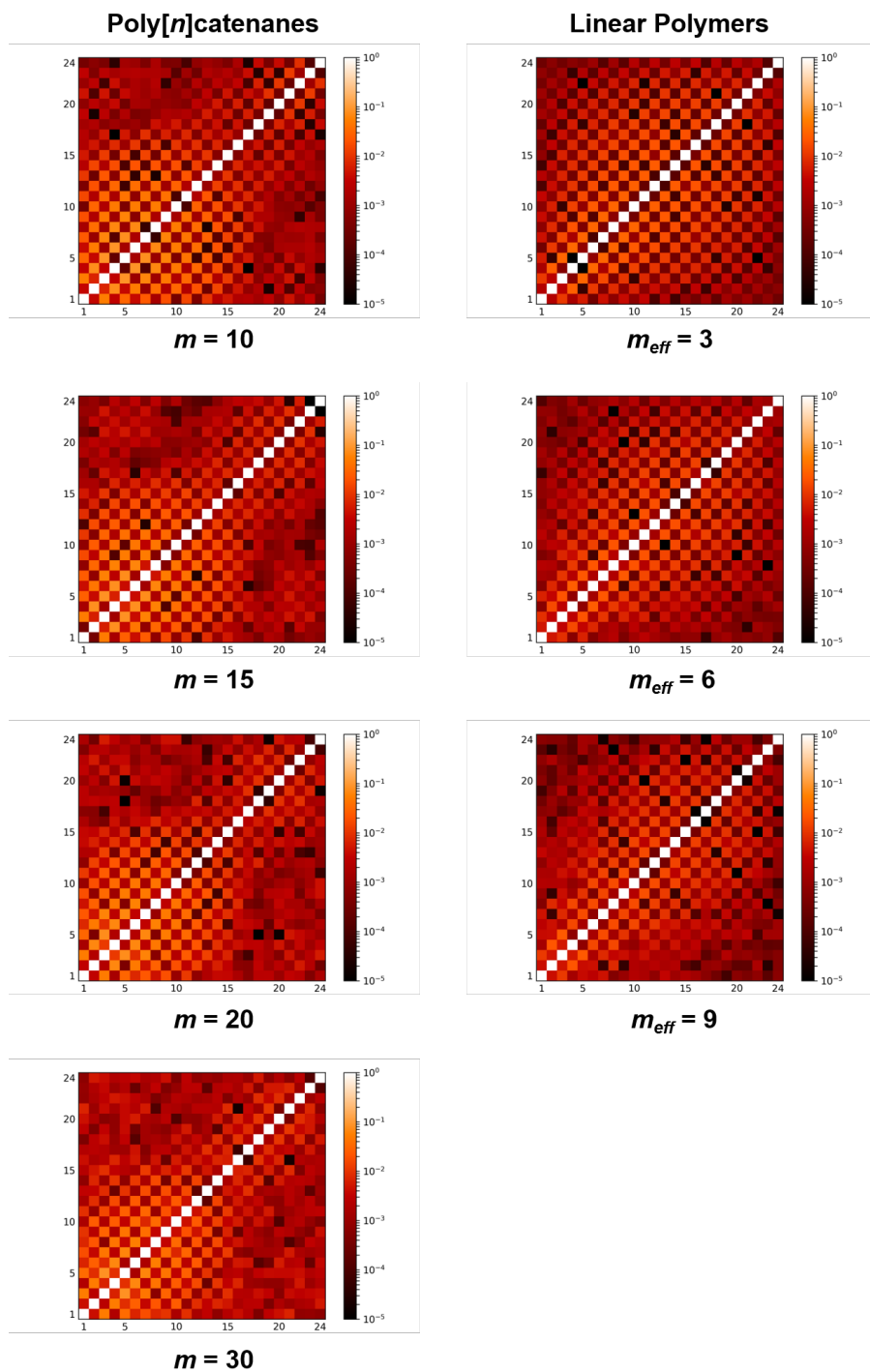


Figure S6: Normalized correlations between Rouse modes of poly[n]catenanes and linear polymers.

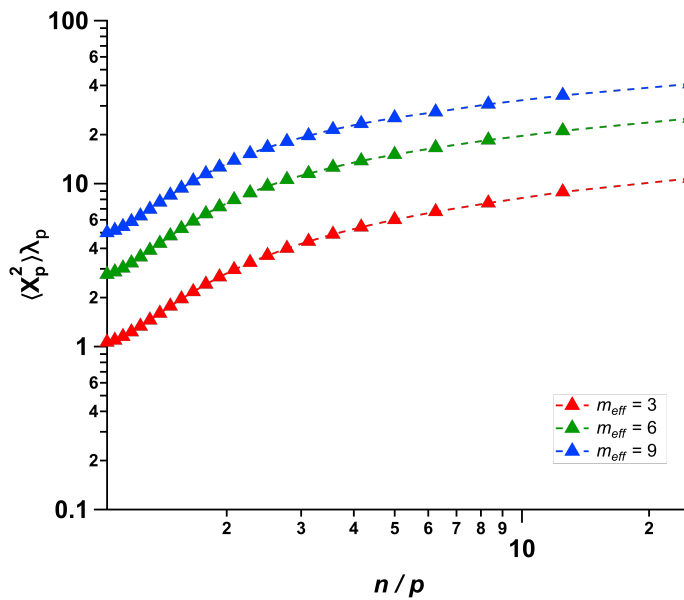


Figure S7: Scaled Rouse mode amplitudes for linear polymers.

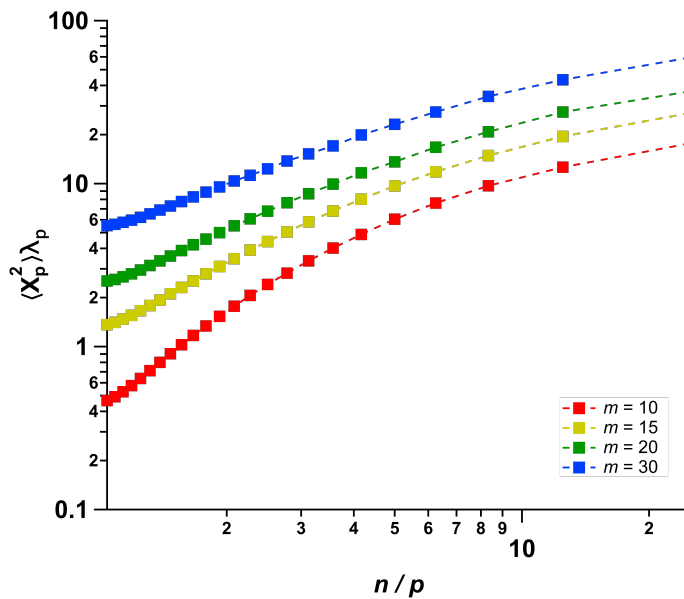


Figure S8: Scaled Rouse mode amplitudes for poly[n]catenanes.

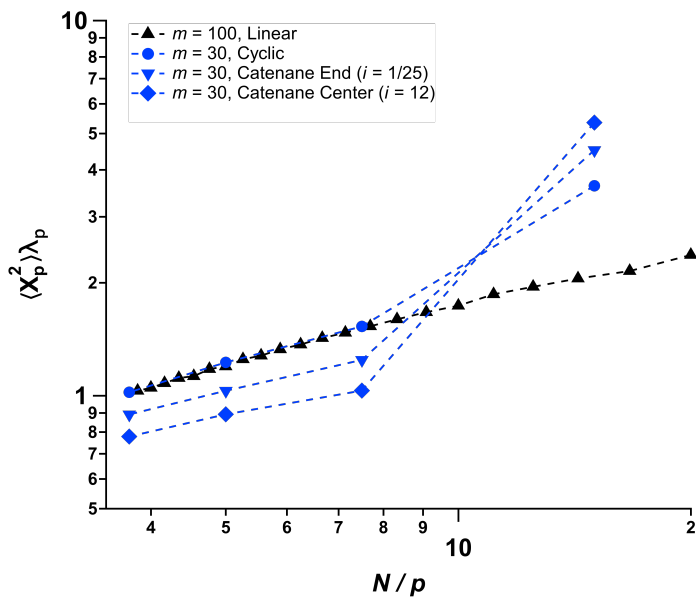


Figure S9: Scaled Rouse mode amplitudes for macrocycles within poly[n]catenanes ($m = 30$), compared to free ring polymers and linear chains.

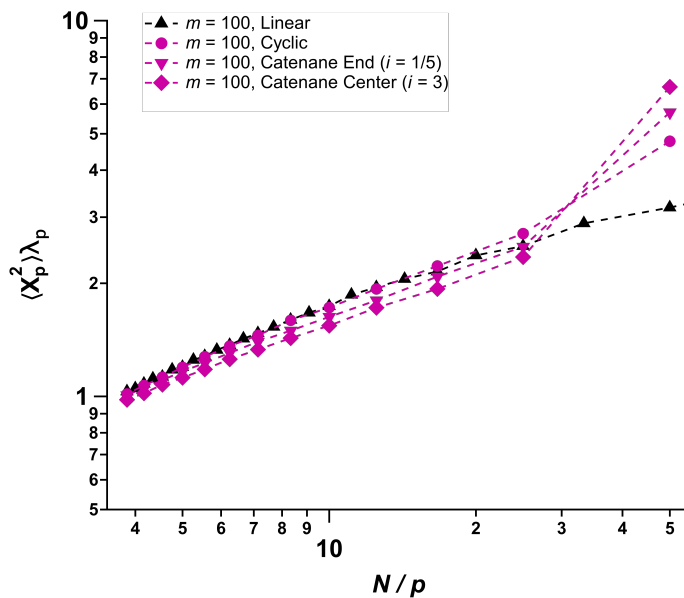


Figure S10: Scaled Rouse mode amplitudes for macrocycles within poly[n]catenanes ($m = 100$), compared to free ring polymers and linear chains.

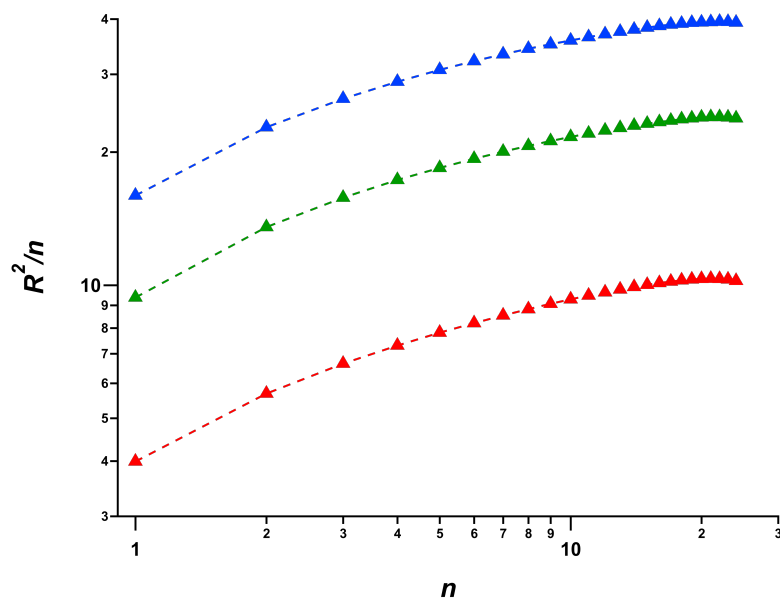


Figure S11: Mean squared internal distances between effective monomers for linear polymers of effective monomer size $m_{eff} = 3$ (red), 6 (green), and 9 (blue). The values increase throughout the range of the function, indicating that these chains are not large enough to reach the asymptotic limit. The tendency to level off also indicates that the chains are locally swollen.

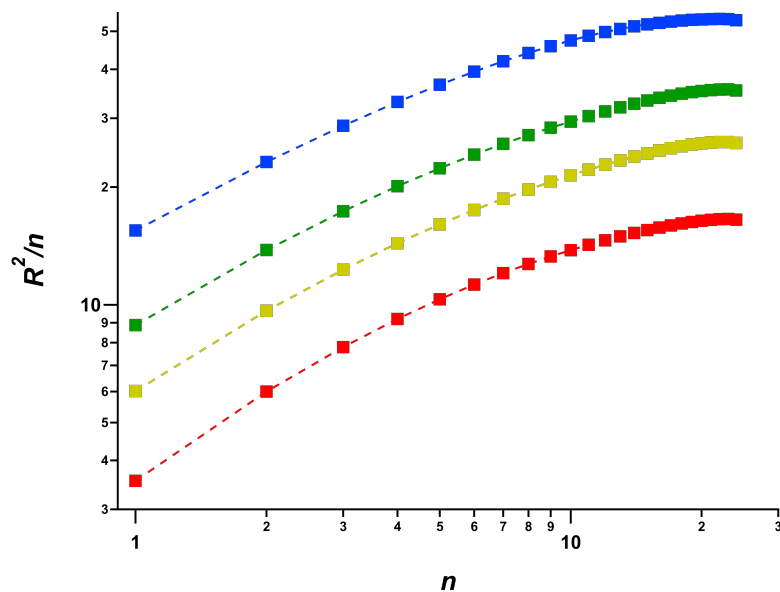


Figure S12: Mean squared internal distances between macrocycles for poly[n]catenanes of ring size $m = 10$ (red), 15 (yellow), 20 (green), and 30 (blue). Similar to linear chains, these polymers are locally swollen and are not large enough to reach a clear asymptotic limit.

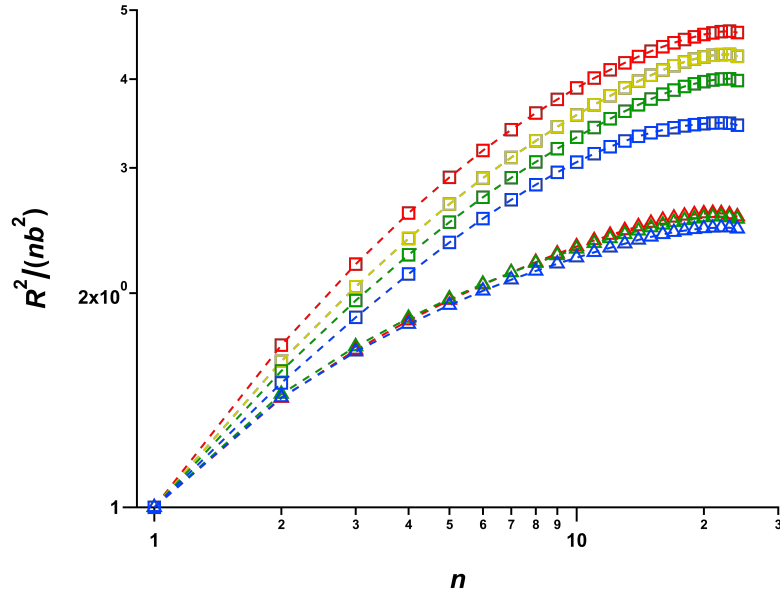


Figure S13: Scaled mean squared internal distances between macrocycles for poly[n]catenanes and linear analogues. The linear polymers (triangles) collapse to a master curve, but poly[n]catenanes do not, indicating that smaller macrocycle sizes lead to greater excluded volume effects.

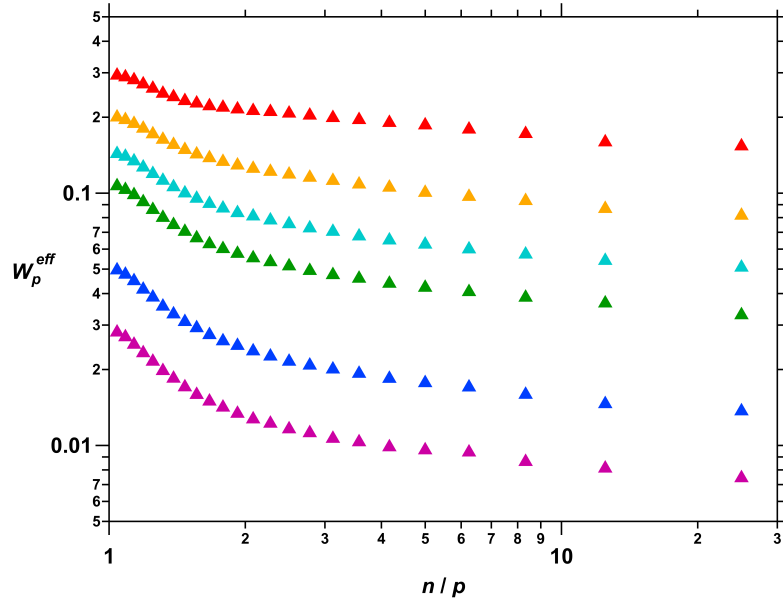


Figure S14: Effective relaxation rates (Eq. S9) for linear polymers with 25 effective monomers of size $m_{eff} = 3$ (red), 4 (orange), 5 (cyan), 6 (green), 9 (blue), 12 (magenta).

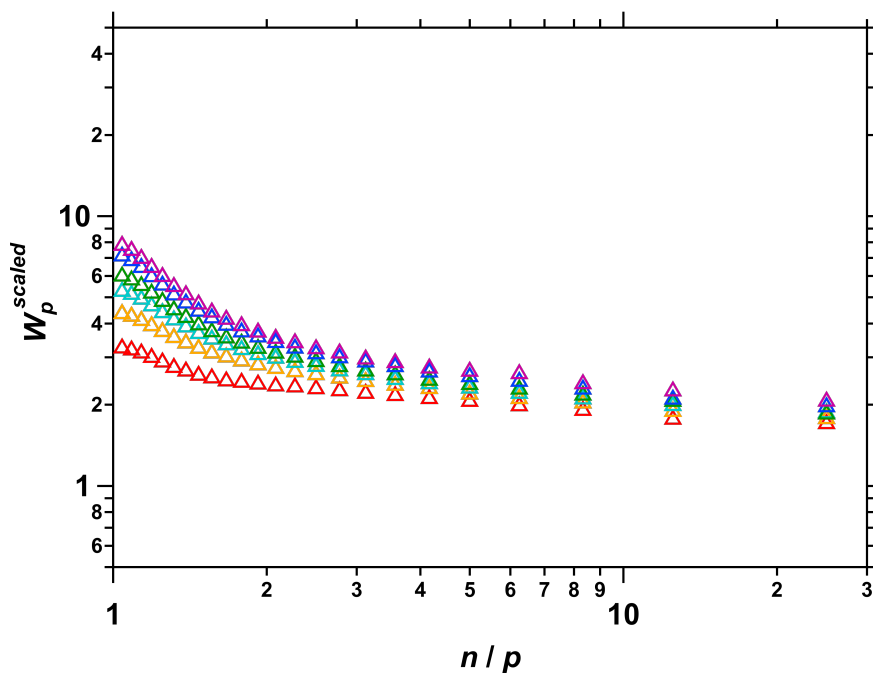


Figure S15: The relaxation spectra of linear polymers from Fig. S14 scaled according to Eq. S16.

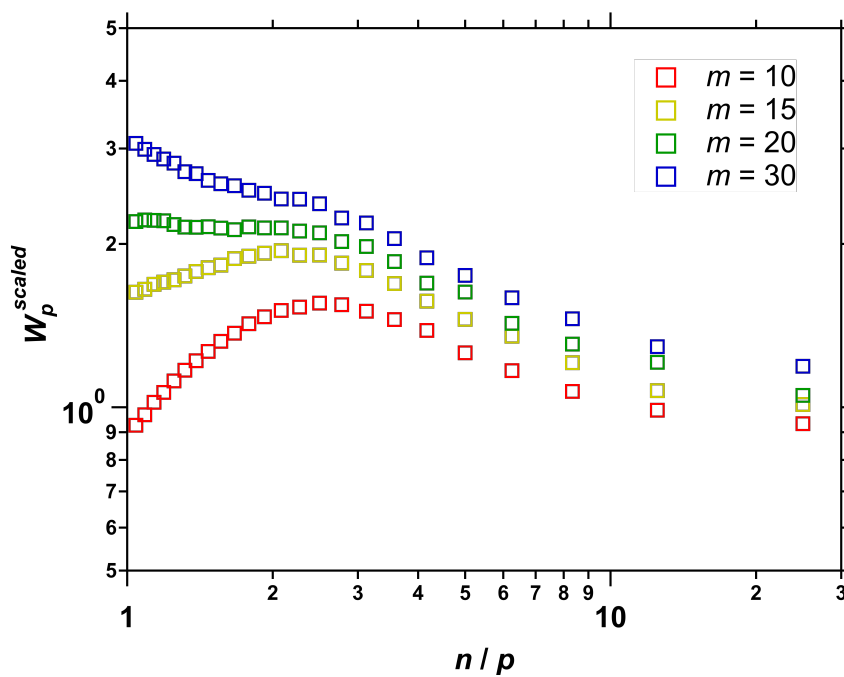


Figure S16: The relaxation spectra for poly[\$n\$]catenanes from Fig.3a scaled according to Eq. S16.

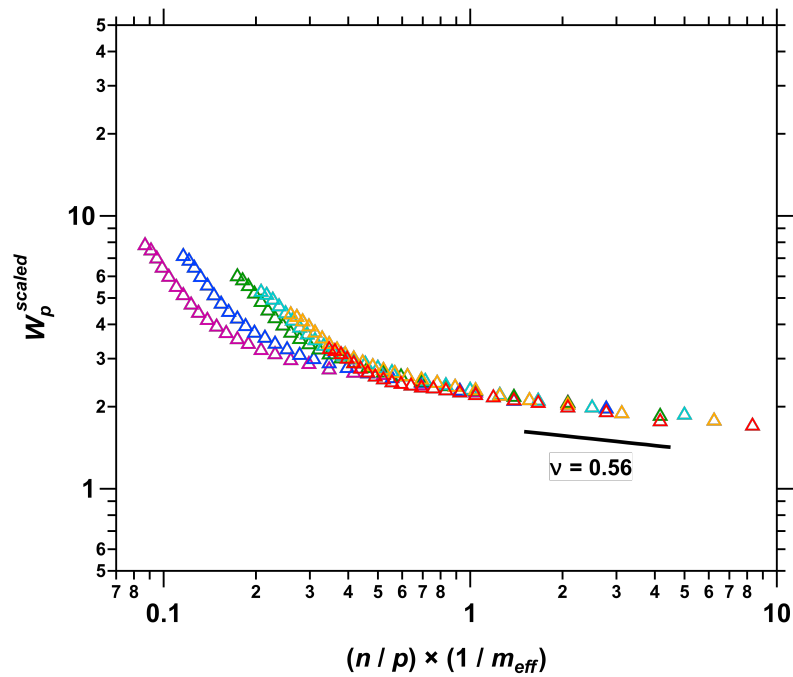


Figure S17: The relaxation spectra for linear polymers from Figure S4 shifted horizontally according to Eq. S24. The slope of the line at low mode number corresponds to a scaling exponent of 0.56, consistent with good solvent conditions.

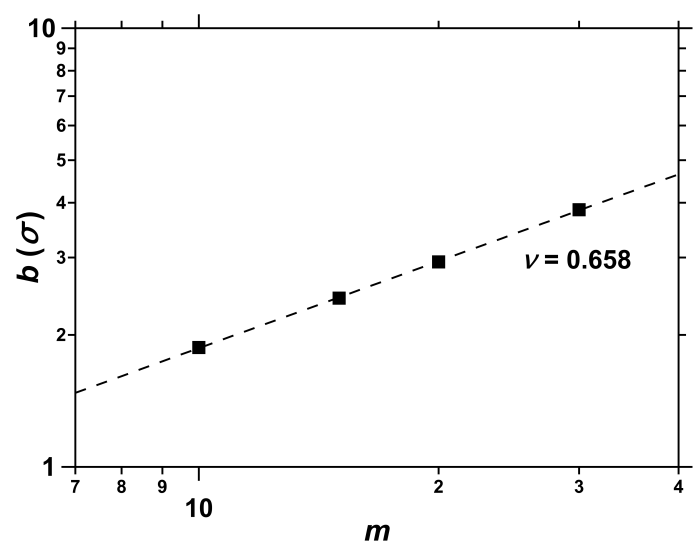


Figure S18: Mean segment length b , as a function of m for poly[n]catenanes. Data points are simulation data; dashed line is a power law fit.

Table S1: Rouse mode stretching exponents, β_p , of various polymer architectures ($m = 100$) as determined from the first Rouse mode analysis described in the main text.

Architecture	$p = 2$	$p = 4$	$p = 6$
Linear Polymer	0.94	0.96	1.05
Ring Polymer	0.90	0.95	0.99
Poly[n]catenane Chain End ($i = 1$)	0.76	0.87	0.90
Poly[n]catenane Chain Center ($i = 3$)	0.69	0.77	0.85

Table S2: Static Properties of Selected Poly[n]catenanes and Linear Analogues

Property	Poly[n]catenane	Linear Polymer
N	250	75
m or m_{eff}	10	3
$b(\sigma)$	1.87	1.90
$\langle R_g^2 \rangle^{1/2}$	7.74	6.25
$\langle R_{ee}^2 \rangle^{1/2}$	19.8	16.0
N	500	150
m or m_{eff}	20	6
$b(\sigma)$	2.93	3.00
$\langle R_g^2 \rangle^{1/2}$	11.5	9.62
$\langle R_{ee}^2 \rangle^{1/2}$	29.4	24.4
N	750	225
m or m_{eff}	30	9
$b(\sigma)$	3.73	3.70
$\langle R_g^2 \rangle^{1/2}$	14.5	12.4
$\langle R_{ee}^2 \rangle^{1/2}$	36.6	31.6

References

- (31) Reid, D. R. *DASH* <http://miccomcodes.org/index.html>.
- (32) Ceriotti, M.; Parrinello, M.; Markland, T. E.; Manolopoulos, D. E. Efficient Stochastic Thermostatting of Path Integral Molecular Dynamics. *J. Chem. Phys.* **2010**, *133*, 124104.
- (33) Kreer, T.; Baschnagel, J.; Müller, M.; Binder, K. Monte Carlo Simulation of Long Chain Polymer Melts: Crossover from Rouse to Reptation Dynamics. *Macromolecules* **2001**, *34*, 1105–1117.
- (34) Downey, J. P. Static and Dynamic Scaling Properties of Single, Self-Avoiding Polymer Chains in Two Dimensions via the Bond Fluctuation Method of Monte Carlo Simulation. *Macromolecules* **1994**, *27*, 2929–2932.
- (35) Panja, D.; Barkema, G. T. Rouse Modes of Self-Avoiding Flexible Polymers. *J. Chem. Phys.* **2009**, *131*, 154903.
- (36) de Gennes, P.-G. Dynamics of Entangled Polymer Solutions. I. The Rouse Model. *Macromolecules* **1976**, *9*, 587–593.
- (37) Ceperley, D.; Kalos, M. H.; Lebowitz, J. L. Computer Simulation of the Dynamics of a Single Polymer Chain. *Phys. Rev. Lett.* **1978**, *41*, 313–316.
- (38) Ceperley, D.; Kalos, M. H.; Lebowitz, J. L. Computer Simulation of the Static and Dynamic Properties of a Polymer Chain. *Macromolecules* **1981**, *14*, 1472–1479.
- (39) Richter, D.; Monkenbusch, M.; Allgeier, J.; Arbe, A.; Colmenero, J.; Farago, B.; Bae, Y. C.; Faust, R. From Rouse Dynamics to Local Relaxation: A Neutron Spin Echo Study on Polyisobutylene Melts. *J. Chem. Phys.* **1999**, *11*, 6107.

- (40) Bennemann, C.; Baschnagel, J.; Paul, W.; Binder, K. Molecular-Dynamics Simulation of a Glassy Polymer Melt: Rouse Model and Cage Effect. *Comput. Theo. Polym. Sci.* **1999**, *9*, 217–226.
- (41) Brodeck, M.; Alvarez, F.; Arbe, A.; Juranyi, F.; Unruh, T.; Holderer, O.; Colmenero, J.; Richter, D. Study of the Dynamics of Poly(ethylene oxide) by Combining Molecular Dynamic Simulations and Neutron Scattering Experiments. *J. Chem. Phys.* **2009**, *130*, 094908.
- (42) Pérez-Aparicio, R.; Colmenero, J.; Alvarez, F.; Padding, J. T.; Briels, W. J. Chain Dynamics of Poly(ethylene-*alt*-propylene) Melts by Means of Coarse-Graining Simulations Based on Atomistic Molecular Dynamics. *J. Chem. Phys.* **2010**, *132*, 024904.